Analysis of Semiconductor Laser-Induced Impurity Activation Using Free Carrier Absorption

K. Ukawa[1], Y. Sakakura[1] T. Sameshima[1], N.Sano[2], M.Naito[3] and N. Hamamoto[3]

[1] Tokyo University of Agriculture and Technology, Koganei, Tokyo 184-8588, Japan
[2] Hightec Systems Corporation, Yokohama, 222-0033, Japan
[3] Nissin Ion Equipment Co., Ltd. Koka, Shiga 528-0068, Japan
E-mail : tsamesim@cc.tuat.ac.jp

Keywords: free carrier absorption, infrared light, microwave, sheet resistance, carrier concentration

Abstract. We report analysis of impurity activation using infrared light and microwave free carrier absorption method. We carried out implantation of boron clusters at 6.0×10^{14} cm^{-2} and 6keV, phosphorus ions at $2.6\times10^{15}cm^{-2}$ and 70keV, and BF_3 ions at $4.4\times10^{14}cm^{-2}$ and 10keV. 200-nm-thick carbon films were formed on the silicon surface as a photo absorption layer using sputtering method. The analysis infrared light absorption revealed that 940-nm-laser irradiation with a diameter of 180 μm at 25 W for 3.6 ms decreased the sheet resistance to 608 Ω/□ in the case of boron clusters. The carrier concentration was estimated to be 5.3×10^{14} cm^{-2} and the activation ratio was 0.89. Microwave absorption analysis also gave decrease in sheet resistance to 564 Ω/□. The sheet resistance and the carrier concentration were 104 Ω/□ and 2.2×10^{15} cm^{-2}, respectively, for phosphorus implantation in the case of laser irradiation for 2.6 ms at 25 W. They were 921 Ω/□ and 4.4×10^{14} cm^{-2} for BF_3 implantation. The PN diodes fabricated in boron cluster doping region showed a characteristic with an ideal factor of 1.42.

Introduction

We have investigated activation of impurity atoms by CW infrared semiconductor laser using carbon layer as a optical absorption layer [1, 2]. Infrared semiconductor laser is attractive to heating process with a high throughput because of its high power of ~10 kW, its high conversion efficiency ~50% and its stable emission. In order to solve the problem of low optical absorbance of Si in the infrared region, carbon was used as absorption layer. Carbon layer has a high optical absorbance and a high thermal durability to temperature around 5000 K. Therefore carbon layer can act as heat source to rapidly heat underlying silicon substrate to a high temperature.

In this paper, we report investigation of electrical properties of impurity doping regions formed by semiconductor laser annealing. We present measurements of infrared light and microwave absorption and its analysis using free carrier absorption theory. Though the experimental and theoretical results, we demonstrate non-destructive and non-contact analysis method of electrical properties of semiconductor, which will be useful during device fabrication. We also report diode properties fabricated in doped region.

Experimental

Boron clusters with a boron concentration of $6.0\times10^{14}cm^{-2}$ were implanted with an acceleration energy of 6keV into n-type silicon substrates with a sheet resistance of 133 Ω/□ and a thickness of 720 μm. Phosphorus atoms with a concentration of $2.6\times10^{15}cm^{-2}$ were also implanted with an acceleration energy of 70keV into p-type silicon substrates with a sheet resistance of 192 Ω/□ and a thickness of 720 μm. Moreover, BF_3 ions with a boron concentration of $4.4\times10^{14}cm^{-2}$ were also implanted with an acceleration energy of 10keV into n-type silicon substrates with a sheet resistance of 85 Ω/□ and a thickness of 720 μm. The total boron and phosphorus concentrations given above were measured by secondary ion mass spectroscopy (SIMS) analysis. The junction depths determined by the depth at an

impurity concentration of $10^{18}cm^{-3}$ were 9, 251 and 48 nm for samples implanted with boron clusters, phosphorus and BF_3, respectively. Then 200-nm-thick carbon films were formed on the silicon surface as a photo absorption layer by the sputtering method. Optical measurement revealed that the optical absorbance was 75 % at 940 nm. Samples mounted on a mobile stage were irradiated with a 940 nm CW infrared semiconductor laser with a power ranging from 21 to 25 W. The laser beam had a diameter of 180 μm at the sample surface and a Gaussian like power distribution. After laser irradiation, the carbon layer was removed by oxygen plasma treatment. Optical spectra in ultra-violet and visible region revealed that the surface region of each samples were completely recrystallized by the laser annealing.

The rear surfaces of the samples were polished for the measurement of infrared transmissivity optical spectra by conventional Fourier transform infrared (FTIR) spectrometry. Experimental spectra were analyzed by fitting process of calculated spectra obtained by a numerical program using free carrier absorption and optical interference theories. The sheet resistance and carrier concentration of the doped layer were estimated. The transmissivities of microwave were also measured using an interferometer-type equipment, as shown in Figure 1 [3]. Sample and reference were inserted in the gaps A and B, respectively. The microwave was introduced using a waveguide and split into two branches by T-type waveguide. Then the microwaves transmitted through the samples were combined. The transmissivity of samples was calculated by the intensities of the sum I_{A+B} and difference I_{A-B} of the microwaves. The detection accuracy of the present system in the transmissivity was ± 0.1 %. The experimental transmissivities were analyzed by numerical finite element program using the free carrier absorption theory. Diodes were fabricated to evaluate electrical properties of pn junction.

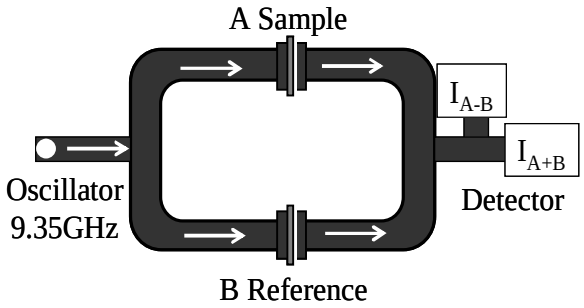

Fig. 1: Schematic equipment of the free carrier absorption measurement system

Free Carrier Absorption

The free carrier absorption effect is explained by the Drude theory. The real part ε_r and the imaginary part ε_i of the complex dielectric constant are expressed as,

$$\varepsilon_r = n_f{}^2 - \kappa_f{}^2 = \varepsilon_{Si} - \frac{\omega_p^2 \tau^2}{1+\omega^2\tau^2} \quad (1),$$

$$\varepsilon_i = 2 n_f \kappa_f = \frac{\omega_p^2 \tau}{\omega(1+\omega^2\tau^2)} \quad (2)$$

, where, ω is the angular frequency, ε_{si} is the dielectric constant of intrinsic silicon, n_f is the refractive index of silicon, k_f is the extinction coefficient induced by free carrier optical absorption, τ is the lifetime of carriers and ω_p is the plasma angular frequency, which is proportional to square root of the carrier density. In the microwave case, ω is 9.35 GHz and $\omega^2\tau^2$ is much lower than 1. ε_r and ε_i are therefore approximated as,

$$\varepsilon_r \sim \varepsilon_{Si} - \omega_p^2 \tau^2 \quad (3),$$

$$\varepsilon_i \sim \frac{\omega_p^2 \tau}{\omega} \quad (4).$$

ε_r is lower than the initial value by $\omega_p{}^2\tau^2$, and does not depend on the microwave angular frequency. ε_i can be very high for low ω, the free carrier absorption is sensitively observed at the 9.35 GHz microwave frequency. ε_i is also proportional to the electrical conductivity (product of the carrier density and the carrier lifetime).

On the other hand $\omega^2\tau^2$ is generally much higher than 1 for frequencies in infrared regions. They are approximated as follows,

$$\varepsilon_r \sim \varepsilon_{Si} - \frac{\omega_p^2}{\omega^2} \quad (5),$$

$$\varepsilon_i \sim \frac{\omega_p^2}{\omega^3 \tau} \quad (6).$$

ε_r is lower than the initial value by ω_p^2/ω^2, and does not depend on the carrier lifetime. Although ε_i is low because of the high angular frequency, it is interesting that ε_i increase as τ decreases. FTIR measurement will be suitable for analysis of free carrier effect of heavy doped layers with a low carrier lifetime, low carrier mobility as well as a high carrier density. Eqs. (5) and (6) mean that the carrier mobility and carrier density can be determined by analysis of FTIR spectra with different angular frequencies.

Figure 2 shows calculated transmissivity and absorbance of a 9.35 GHz microwave as well as for 45 THz infrared light (1500 cm^{-1}) as a function of the sheet resistance for a 10nm p-type doped layer formed in n-type silicon substrates with a substrate sheet resistance of 133 Ω/□ and a thickness of 720 μm. For the infrared case, transmissivity and absorbance were calculated with two different carrier mobilities of 12.5 and 50.0 cm^2/Vs in the doped layer. The transmissivities of the infrared light and the microwave monotonously decreased for decreasing sheet resistance. The transmissivity at 45THz (1500cm^{-1}) for a mobility of 12.5 cm^2/Vs decreased much more than that for 50.0 cm^2/Vs. There is substantial absorbance of the microwave caused by free carriers in silicon substrate. The absorbance of the microwave monotonously decreased as the sheet resistance in the top doped region decreased because the reflectivity increased as the sheet resistance decreased. On the other hand, there is an absorbance peaks of infrared light at 90 Ω/□ for 12. 5cm^2/Vs and 25 Ω/□ for 50.0 cm^2/Vs. The peak

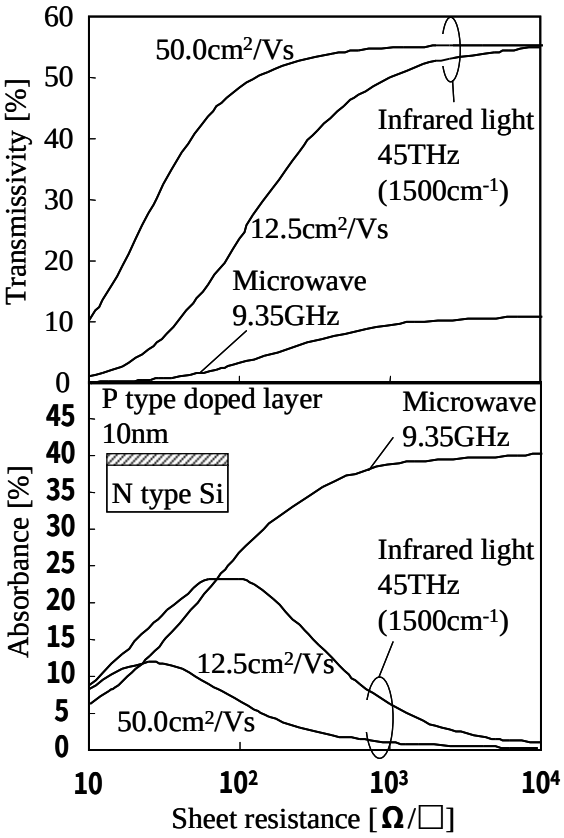

Fig. 2 . Calculated absorbance and transmissivity of a 9.35 GHz microwave as well as for 45 THz infrared light (1500 cm^{-1}) as a function of the sheet resistance for a 10 nm p-type doped layer on n-type silicon substrates with a sheet resistance of 133 Ω/□ and a thickness of 720 μm.

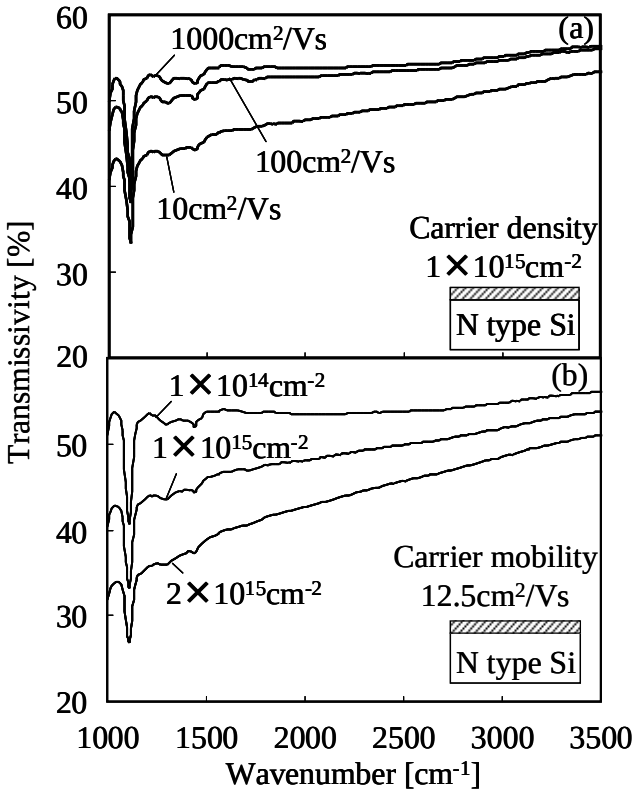

Fig. 3. Calculated transmissivity spectra in infrared region of a doped layer for different carrier mobilities and a carrier density of 1×10^{15} cm^{-2} (a) as well as for different carrier concentrations and a carrier mobility of 12.5 cm^2/Vs (b).

absorbance for 12.5cm^2/Vs was higher than that for 50.0cm^2/Vs according to serious change in the dielectric constant.

Figure 3 shows calculated transmissivity spectra in infrared region for different carrier mobilities (a) as well as for different carrier concentrations (b) in the doped layer. The transmissivity decreased as the carrier mobility decreased as shown in figure (a) according to high optical absorption given by eq (6). It also decreased as the carrier concentration increased as shown in figure (b). The fitting process of calculated spectra to experiment ones gives values of carrier mobility and carrier concentration.

Results and Discussion

Figure 4 shows the FTIR transmissivity spectra of the samples as-implanted and the laser irradiated for implantations of boron clusters at 6 keV. Laser irradiations at 21 and 25 W for 3.6 ms were conducted**.** Calculated spectra are also plotted in Fig.4. The calculated spectra were obtained by a numerical program using free carrier absorption and optical interference theories. The carrier distribution obtained by a finite element method was also used in calculation of transmissivity spectra. The transmissivity decreased especially in the low wavenumber region because of high free carrier absorption effect for laser annealed samples. Especially it was low in the case of laser annealing at 25 W. Agreement between experimental and calculated spectra gave sheet resistance, carrier density and carrier mobility for doped region as shown in Fig.5. The sheet resistance decreased from 987 to 608 Ω/□ as the laser power intensity increased from 21 to 25 W. Our analysis resulted in the fact that the carrier concentration markedly increased from 2.9×10^{14} to 5.8×10^{14} cm^{-2} as laser power intensity increased. Heating at high temperature effectively generated hole carriers. The activation ratio was turned out to be 0.89 for a laser power of 25 W.

Figure 6 shows the transmissivity of microwave for the laser irradiated samples for laser powers of 21 and 25 W, which were the same samples measured by FTIR. The transmissivity of microwave were also analyzed and the sheet resistance of the doped layer was estimated. They were presented in the horizontal axis in Fig.6. The calculated curve of the transmissicity as a function of sheet resistance was also plotted in Fig.6. The transmissivity of microwave and the sheet resistance decreased from 9.2 to 8.4% and 856 to 564 Ω/□, respectively, as the laser power intensity increased from 21 to 25 W. Effective carrier generation was also observed by the microwave absorption method. The analyzed sheet resistances were also presented in Fig.5 for comparison to FTIR results. There was rather good agreement between values given by both methods. The carrier density was also presented when the carrier mobility obtained by FTIR method was used.

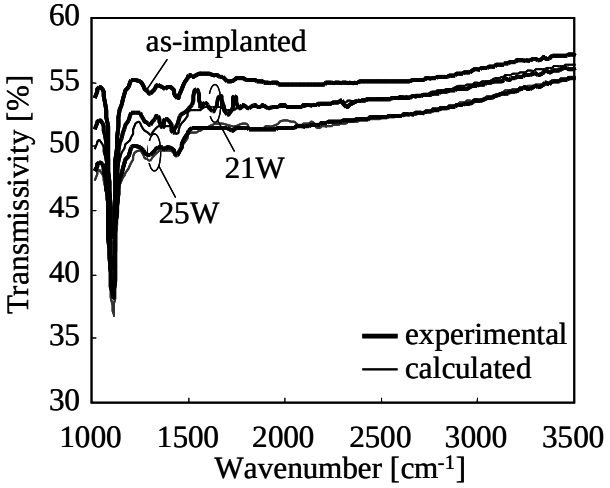

Fig. 4. The transmissivity spectra of the samples as-implanted and the laser irradiated for implantation of boron clusters at 6 keV measured by FTIR. The calculated spectra are also shown.

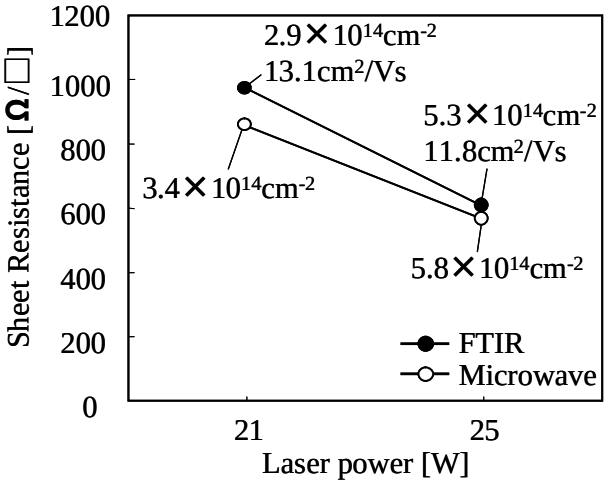

Fig. 5. Sheet resistance of doped layer analyzed by infrared light and microwave free carrier absorption methods of the samples as-implanted and the laser irradiated for implantation of boron clusters at 6keV as a function of laser power. Carrier concentration and carrier mobility are also shown.

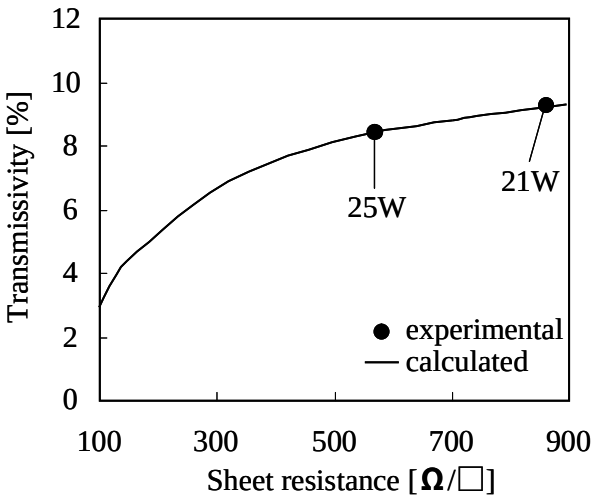

Fig. 6. The transmissivity of microwave of the laser irradiated samples for implantation of boron clusters at 6 keV as a function of the sheet resistance of the doped layer. Calculated transmissivity is also shown.

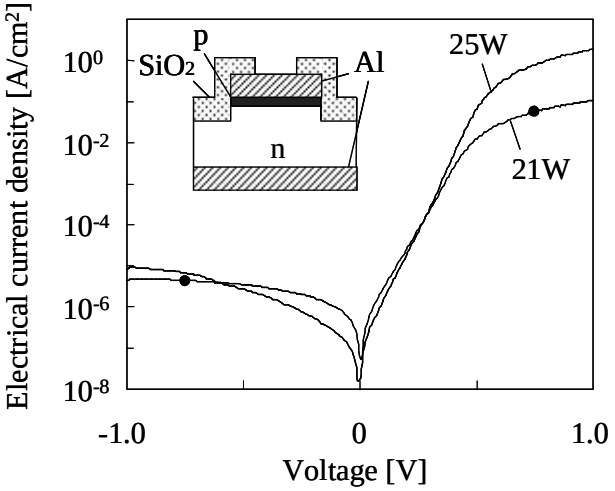

Fig. 7. Electrical current as a function of voltage for pn diodes formed in the laser irradiated regions for implantation of boron clusters at 6 keV.

To evaluate the pn junction, the diodes with the mesa structure as shown by inset in Fig. 7. I-V characteristics of pn junction formed for the laser irradiated samples for implantations of boron clusters at 6keV are presented in Fig.7. The ideality factor and the reverse bias current were 1.80 and 4.7μA/cm^2 for 21 W, and 1.42 and 8.6μA/cm^2 for 25 W, respectively. This result revealed that a heavily doped layer with a thin depth was well activated with a low defect density by CW infrared semiconductor laser irradiation.

Figure 8 shows the FTIR transmissivity spectra of the samples as-implanted and laser irradiated for implantations of phosphorus at 70 keV (a) and of BF_3 ions at 10keV (b). Laser irradiations at 25 W for 1.2 and 2.6 ms were conducted. The transmissivity decreased by laser annealing. Calculated spectra were also plotted and they agreed well to the experimental ones. The spectra were almost same between laser irradiation for 1.2 and 2.6 ms for phosphorus and BF_3 doping cases. It indicates the laser dwell time of 1.2 ms was enough and dopant atoms were well activated. Figure 9 shows our precise analyses of sheet resistance, carrier concentration and carrier mobility. Sheet resistance slightly decreased from 121 to 104 Ω/□ as the dwell time increased 1.2 to 2.6 ms for phosphorus doping because the carrier

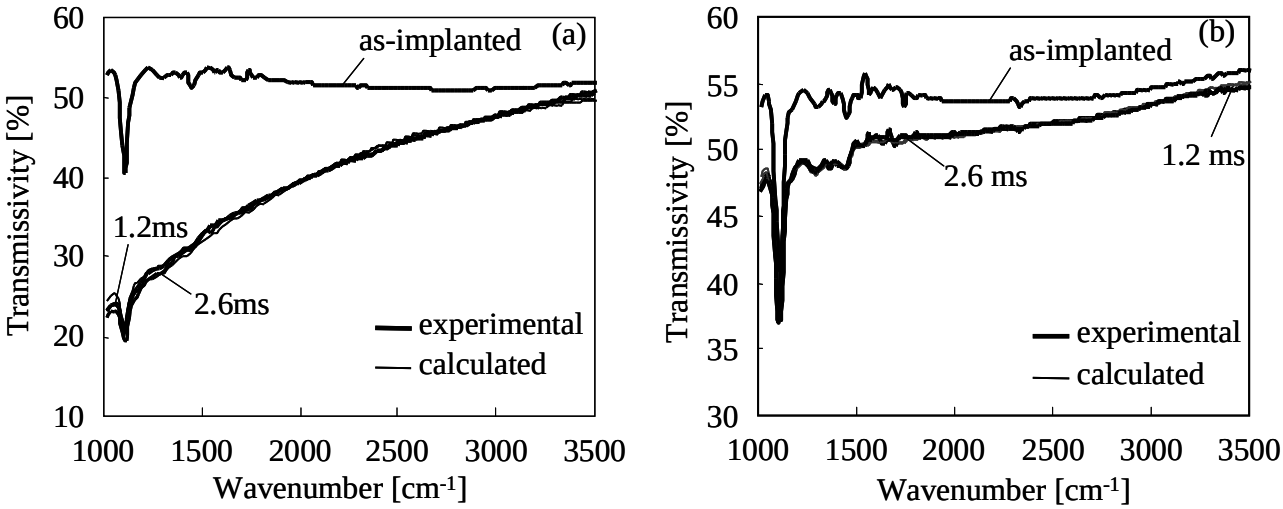

Figure 8. The transmissivity spectra of the as-implanted sample and the laser irradiated samples for implantations of phosphorus atoms at 70 keV (a) and BF_3 ions at 10keV (b) measured by FTIR. The calculated spectra are also shown.

concentration and the carrier mobility slightly increased from 2.1×10^{15} to 2.2×10^{15} and 24.4 to 26.4 cm^2/Vs, respectively. The slight decrease in sheet resistance was also observed in BF_3 doping from 945 to 921 Ω/□, which resulted from increase in the carrier concentration from 4.2×10^{14} to 4.4×10^{14}. The activation ratio for 2.6 ms for phosphorus and BF_3 were estimated to be 0.83 and 1.0, respectively. These results indicate that low annealing has an advantage of carrier generation, although the changes in those values with laser dwell time are close to our resolution limit.

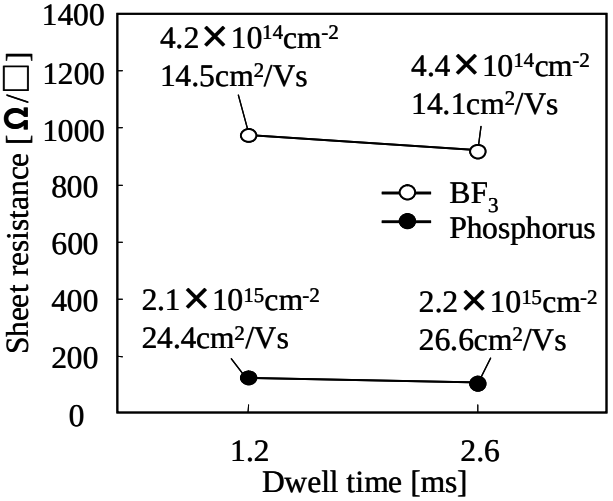

Figure 9. Sheet resistance of doped layer analyzed by infrared light free carrier absorption method for implantations of phosphorus atoms at 70 keV as well as BF_3 ions at 10keV as a function of dwell time. Carrier concentration and carrier mobility are also shown.

Summary

We report analysis of impurity doping using infrared light and microwave free carrier absorption method. We carried out implantation of boron clusters at 6.0×10^{14} cm^{-2} and 6keV, phosphorus ions at $2.6\times10^{15}cm^{-2}$ and 70keV, and BF_3 ions at $4.4\times10^{14}cm^{-2}$ and 10keV. 200-nm-thick carbon films were formed on the silicon surface as a photo absorption layer using sputtering method. The samples were irradiated with a 940 nm CW infrared semiconductor laser with a beam diameter of 180 μm to activate impurity atoms. Laser irradiations with a laser power of 21 and 25 W for 3.6 ms were conducted to the samples for implantations of boron clusters at 6keV. The sheet resistance decreased from 987 to 608 Ω/□ as the laser power intensity increased from 21 to 25 W. The carrier concentration markedly increased from 2.9×10^{14} to 5.8×10^{14} cm^{-2} as laser power intensity increased. The activation ratio for 25 W was estimated to be 0.89. With microwave free carrier absorption analysis the sheet resistance decreased from d 856 to 564 Ω/□. The diodes were fabricated with the mesa structure. The ideality factor and the reverse bias current were 1.80 and 4.7μA/cm^2 for 21 W, and 1.42 and 8.6μA/cm^2 for 25 W, respectively. This result revealed that a heavily doped layer with a thin depth was well activated with a low defect density by CW infrared semiconductor laser irradiation. Laser irradiations with a laser power of 25 W for 1.2 and 2.6 ms were conducted to the samples for implantations of phosphorus atoms at 70keV as well as BF_3 ions at 10keV. Sheet resistance slightly decreased from 121 to 104 Ω/□ as the dwell time increased 1.2 to 2.6 ms for phosphorus doping owing to the slight increases in carrier concentration and carrier mobility. The slight decrease in sheet resistance was also observed in BF_3 doping from 945 to 921 Ω/□ owing to the slight increase in carrier concentration. The activation ratio for 2.6 ms for phosphorus and BF_3 were estimated to be 0.83 and 1.0, respectively.

Acknowledgement

This work was partially supported by CASIO Science Promotion Foundation.

REFERENCEES

[1] N.Sano, N. Andoh and T. Sameshima, Y. Matsuda, and Y. Andoh, Jpn. J.Appl. Phys. 46 (2007) L620-L622.
[2] T.SAMESHIMA,M.MAKI, M.TAKIUCHI, N. ANDOH, N. SANO, Y. MATSUDA and Y. ANDOH, Jpn. J.Appl. Phys. 46 (2007) pp. 6474-6479.
[3] T. Sameshima, H. Hayasaka, and T. Haba, Proc. in Workshop on Active Matrix Flat Panel Displays (Tokyo, 2008) p205-208